Effect of Travel Speed on Quality and Welding Efficiency of Friction Stir Welded AZ31B Magnesium Alloy

Amir Hossein Baghdadi[1], Nor Fazilah Mohamad Selamat[1], Zainuddin Sajuri[1*] and Amir Hossein Kokabi[2]

[1]*Centre for Materials Engineering and Smart Manufacturing*
Faculty of Engineering and Built Environment
Universiti Kebangsaan Malaysia, 43600 Bangi, Malaysia
[2]*Department of Materials Science and Engineering*
Sharif University of Technology, Tehran, Iran
Corresponding author Email: zsajuri@ukm.edu.my

Abstract

Weight reduction is one of the most concerning issues of automotive and aircraft industries in reducing fuel consumption. Magnesium (Mg) alloys are the lightest alloys which can be used in the structure due to low density and high strength to weight ratio. Developing a reliable joining process of magnesium alloys is required due to limited ductility and low workability at room temperature. Friction stir welding (FSW) is a solid-state welding process that can be performed to produce sound joints in magnesium alloys. Researchers have performed investigations on the effect of rotation and travel speeds in FSW of AZ31B magnesium alloy. However, there is lack of study on the FSW parameters, i.e. travel speed below 50 mm/min and rotation speed lower than 1000 rpm. In this research, FSW of AZ31B magnesium alloy was performed at a constant rotation speed of 700 rpm and varied travel speeds below 50 mm/min. The results showed the development of finer grain size in stir zone with increasing of welding travel speed from 20 mm/min to 40 mm/min. It was found that the finer grain size improved the mechanical properties while maintaining the elongation at different welding parameters.

Keywords: *Automotive industry, AZ31B Magnesium alloy, Friction stir welding, Mechanical properties.*

1. Introduction

Nowadays, weight reduction is one of the most concerning issues in the automotive industry which can significantly reduce fuel consumption and CO2 emission [1-4]. The challenges in manufacturing to reduce vehicle weight are; application of lightweight materials such as high strength steels, aluminium and magnesium alloys, and plastic materials; new structural lightweight construction; and optimizing the design and production processes [4]. Among the challenges, use of lightweight materials is one of the key factors considered for car manufactures, and magnesium alloys are on the list [1, 3]. Magnesium (Mg) alloys are the lightest alloys which can be used for different parts of the body structure and components due to low density and high strength to weight ratio [2]. Furthermore, good castability, excellent machinability, electromagnetic interference shielding properties, good sound damping capability and recyclability are other advantages of magnesium alloys. However, Mg alloys have limited ductility and low workability at room temperature because of their hexagonal closed packed (HCP) crystal structure which resulted in the lack of slip planes in their structures. Therefore, developing a reliable joining process for these applications is required. However, there are still many difficulties in joining Mg alloys to other materials, especially in fusion welding processes such as cracks, oxide inclusions, distortions, and porosity which is common in the welding zone. Friction stir welding (FSW) is a solid-state welding process invented by TWI in 1991 that can be performed to produce sound joints in magnesium alloys [5-7]. During the FSW process, the complex thermo-mechanical input results in microstructure

modification in the weld zone and generates distinct microstructural areas: the nugget, the thermo-mechanically affected zone (TMAZ), the heat affected zone (HAZ) and the base metal. Various researches has been performed to investigate the effect of FSW parameters such as rotation speed, travel speed and applied force on microstructures and mechanical properties such as hardness and tensile properties [8-12]. Abbasi et al. [8] mentioned the effect of rotation and travel speed as ratio parameter of on the microstructure and mechanical properties of the AZ31 alloy where the mechanical properties will slightly decrease with the increase of the ω/υ ratio. Afrin et al. [9] reported that with the increase of the welding speed, the smaller grain size of the AZ31 alloy has been observed in the stir zone (SZ) and tensile properties i.e., ultimate and yield stress values increased due to lower heat input. Besides that, increased in microhardness and grain refinement was observed in the weld zone of the AZ31 alloy by Wang et al. [10], although lower hardness and smaller grain size were reported by Hirano et al. [11] for a dissimilar joint of magnesium and aluminium alloys. In addition, the effects of different FSW parameters on the mechanical properties of the AZ31 alloy were reported by Lee et al. [5], where they found that increases in travel speed of 87 mm/min to 507 mm/min caused the decreasing of tensile strength. Meanwhile, Lim et al. [12] stated that there were no significant effects of the processing parameters on the tensile properties of the FSWed AZ31-H24 magnesium alloy.

Welding rotation and travel speed are considered as main sources of the heat input in FSW. From the above literature reviews, low heat input results in higher mechanical properties due to finer grain size in the microstructure of welding zone. Most of the researches done on FSW of AZ31B were in the high travel speed

between 60 mm/min and 507 mm/min. However, Abbasi et al. [8] have performed FSW of AZ31 in the range lower than 60 mm/min with the welding rotation speed varies between 950 rpm to 1400 rpm. To the best of authors' knowledge, there is no study on the effect of low heat input under the welding travel speed below 50 mm/min and rotation speed lower than 1000 rpm on welding efficiency of AZ31B magnesium alloy. In this study, the effect of low travel speed conditions was investigated through microstructure observation, microhardness, and tensile properties of friction stir welding of AZ31B magnesium alloy.

2. Experimental Procedure

An AZ31B magnesium alloy sheet with a dimension of 150×50×4 mm3 is used in this research as the base metal with the alloy composition mentioned in Table 1 which was measured by X-ray fluorescence (XRF) spectroscopy. Prior to FSW, the surface oxides were removed by steel brush and then the surface was cleaned using ethanol. Fig.1 shows the joint configuration and welding direction.

Table 1: Chemical compositions of as-rolled AZ31B Mg alloy. (wt%)

| Al	Zn	Mn	Mg
2.5-3.5	0.7-1.4	0.2-1.0	Balance
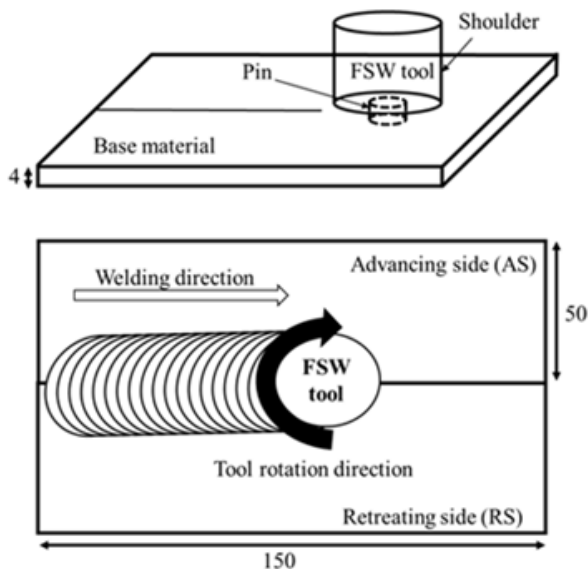
Fig. 1: Joint design and dimensions. (millimetre)

The welding direction is perpendicular to the rolling direction of the AZ31B alloy. The FSW tool with a cylindrical threaded M5 pin was made of heat treated H13 tool steel with a hardness of 53-55 HRC. Fig. 2 shows the schematic view of the FSW tool pin with 3-degree tilled angle of the tool axis during the welding process. First, the tool was gradually pushed into the base metal sheet at a constant rotation speed until the shoulder tip penetrated 0.2 - 0.3 mm to the base metal. Then, the tool was stirred along the joint. Tool rotation speed was set at 700 rpm, and travel speeds of the tool were varied from 20 to 40 mm/min to give a low heat input during the FSW process. Microstructure observation was performed on the cross-section perpendicular to the welding direction. Then, samples were cold mounted, manually ground using #600 to #2000 grit emery papers and polished by Al203 suspensions with the particle size of 1, 0.3, and 0.05 micron, respectively. An etching solution consisting of 10 ml acetic acid, 6 g picric acid, 10 ml distilled water and 100 ml ethanol was used to reveal the microstructure. Microstructures of the stir zone (SZ) and the thermomechanically affected zone (TMAZ) were observed by an optical microscope (OM). Average grain size was measured based on the ASTM standard E112-10.
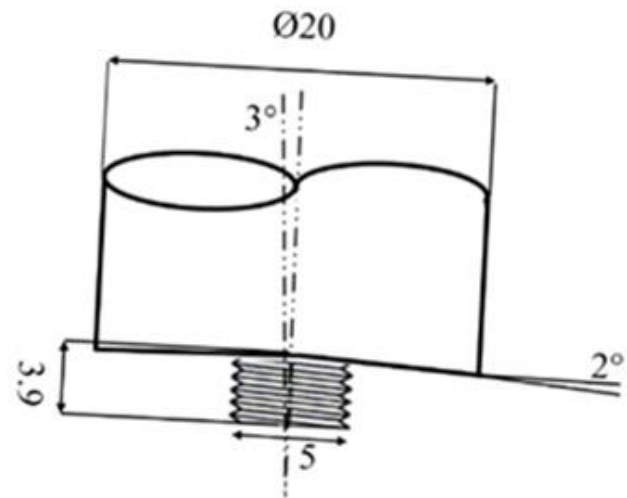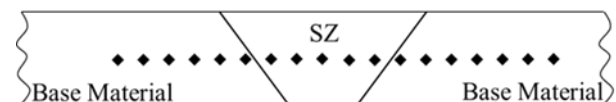
Fig. 2: Schematic representation of welding tool. (millimetre)

Evaluations of the mechanical properties of FSWed AZ31B were performed based on tensile and microhardness tests. The tensile test was performed at ambient temperature (25 °C) with speed of 0.5 mm/min using a specimen with gauge length and width of 40 mm and 6 mm, respectively. The specimen was cut so that the axial loading direction was perpendicular to the welding direction as shown in Fig. 3. The tensile sample was cut according to ASTM E8/E8M standard. The microstructure and fracture surface of the tensile samples were investigated using a scanning electron microscope (SEM) with a voltage of 15 kV equipped with an energy dispersive X-ray spectroscopy (EDS) system. A microhardness test was performed in the middle of the thickness (refer Fig. 4) using a Shimadzu microhardness tester with conditions of 100 g and dwell time of 15 seconds.
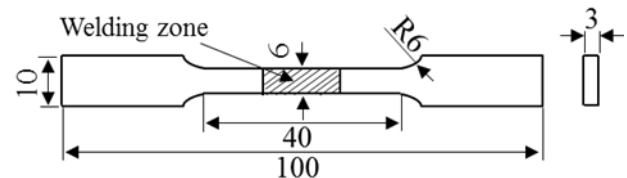
**Fig. 3:** Schematic representation of tensile test specimens. (millimetre)

Fig. 4: Schematic representation of hardness test on welded specimens.

3. Results and Discussion

Figure 5 depicts the FSWed AZ31B samples' surfaces. There was no evidence of crack and porosity on the welded sample's surface and the samples possessed a flash size of less than 2 mm, termed as a sound weld. Furthermore, the weld bead and flash adjacent to the weld beads were reduced with greater welding travel speed of 20 to 40 mm/min. Fig. 6 shows the characteristic of the cross-sectional profile of the stir zone (SZ) of FSWed AZ31B sample. With varying welding travel speeds, joints without defects were fabricated. Microstructures of various welding zones (TMAZ, SZ, and base metal) were noted to be similar to prior studies by Afrin et al. [9], Lim et al. [12], and Yang et al. [13].

The microstructure of AZ31B base metal is exhibited in Fig. 7(a). The base metal microstructure showed the Mg alloys' characteristic rolled microstructure with non-uniform grains and multiple twins. The average grain size of base metal was noted to be around 78 μm. Fig. 7(b)-(d) demonstrates the stir zone microstructures of FSWed AZ31B along with different welding travel speeds.
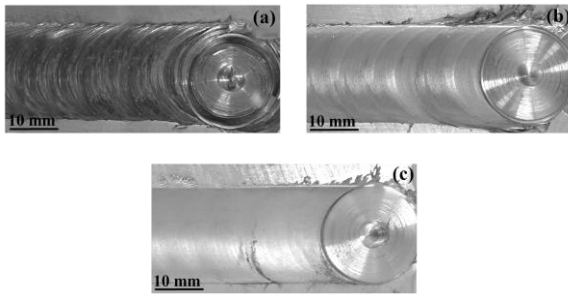
Fig. 5: Digital image of weld surfaces in 700 rpm constant rotation speed: (a) sample 1 - 20 mm/min, (b) sample 2 - 30 mm/min, and (c) sample 3 - 40 mm/min.
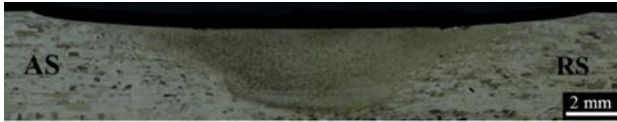
Fig. 6: Typical cross-section photograph of FSWed AZ31B sample (700 rpm, 40 mm/min).

The heat input within the weld area was observed to be impacted by welding conditions such as welding travel speed, rotational speed, and axial force. Usually, low frictional heat input is produced at a lower rotational speed, greater welding travel speed, and lower axial force compared to the opposite circumstance [14]. It assumed that severe plastic deformation and frictional heating in the course of FSW drive creation of fine crystallized grains. When dynamic recrystallization is taking place, either increasing the strain rate or reducing the temperature would generate a finer grain structure. The SZs were recognised on the basis of their even and equiaxed grains, suggesting the incidence of dynamic recrystallization.
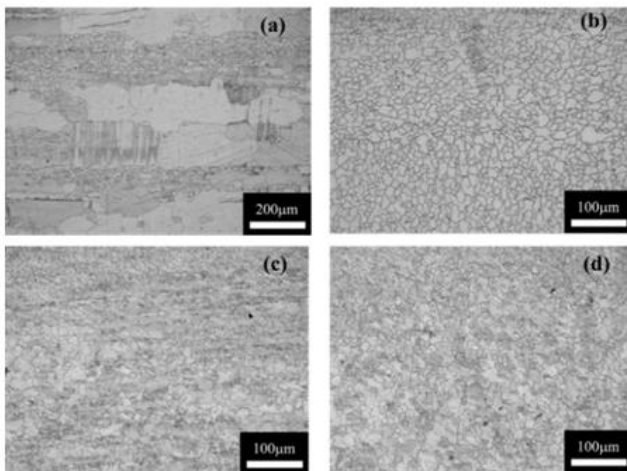
Fig. 7: Microstructure of FSWed AZ31B: (a) base metal, (b) sample 1 - 20 mm/min, (c) sample 2 - 30 mm/min, and (d) sample 3 - 40 mm/min.

For the heat input that was the lowest, along with a welding travel speed of 40 m/min, the SZ grain was the finest at around 10 μm. Reducing the welding travel speed to 30 and 20 mm /min exhibited that the high heat input caused a rise in the average SZ grain size to around 12 and 14 μm (see Table 2). Furthermore, the twins were hardly noted in the SZs. When the heat input reduces, it is clear that the average grain size would reduce as well. In previous studies, the researchers [10, 15-19] stated that the temperature was greater than the recrystallization temperature revealed to the SZ but lesser than the melting point. Accordingly, the SZ underwent dynamic recrystallization under the tool's stirring effects, brought about fine and equiaxed grains, and triggered the fading of the

Table 2: Welding travel speed used in this study and the average grain size in different zones of FSWed AZ31B.

Sample No.	Rotation Speed (rpm)	Welding Travel Speed (mm/min)	Grain Size in SZ (μm)	Grain Size in TMAZ (μm)
1		20	14.1	17.3
2	700	30	11.8	16.6
3		40	10.6	15.9

twins. A rise in the heat input impacted the greater welding temperature in the SZ in the course of welding. This triggered a rise in the recrystallized grain size because of the coarsening of the newly nucleated grains at greater temperature.

Figure 8 shows the microstructures of TMAZ on the advancing side of the FSWed AZ31B. The TMAZs exhibited roughly equiaxed grains that are extremely similar to the study carried out by Padmanaban and Balasubramanian for the FSW AZ31 magnesium alloy, in which elongated grains besides the flow line were not seen in TMAZs [20]. In the micrographs, the TMAZs' microstructure was different and grainier compared to the base metal and stir zones because of inadequate deformation and thermal exposure as well as lower the recrystallization temperature [19, 21]. Moreover, it was noted that the TMAZ grain size varied in three samples at different welding travel speeds. For samples 1, 2, and 3, the average grain size varied from 17.3 to 15.9 μm. It is believed that the heat input triggered by welding travel speed did not cause much impact on the TMAZ average grain size.
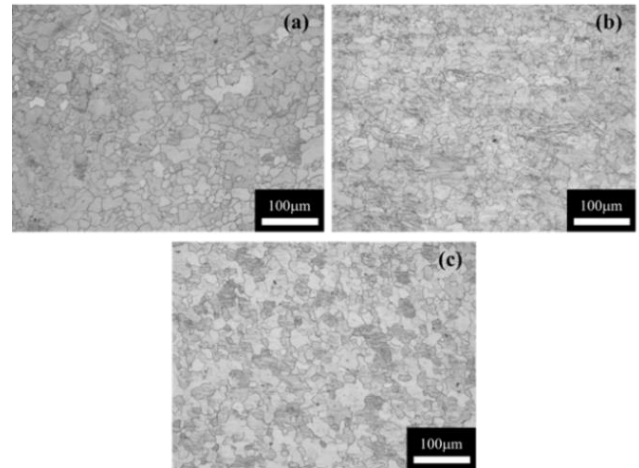

Fig. 8: Microstructure of FSWed AZ31B in TMAZ of advancing side; (a) sample 1 - 20 mm/min, (b) sample 2 - 30 mm/min, and (c) sample 3 - 40 mm/min.

A hardness profile of sample 1, 2, and 3 was performed along the middle of the thickness as shown in Fig. 9. The hardness of the base metal fluctuated due to the inhomogeneous grain microstructure of the as-rolled plate. The average hardness of the base metal was 60 HV. The three FSWed samples showed similar hardness profiles and the hardness value in the SZs was about 60 HV which was corresponding to the base metal value. The AZ31B Mg alloy used in this study does not have a main second phase to control the grain size. Therefore, the hardness value is mainly governed by dislocation density and grain size. However, the hardness profile did not show any notable effect of the average grain size in the different welding regions. This type of profile hardness has also been reported in the previous studies [13, 17, 19]. The sample's post-FSW homogeneous hardness profile was ascribed to the lack of substantial differences in the dislocation density all through the weld [15]. Moreover, J. Yang et al. [13] pointed out that there was no noteworthy difference of the dislocation densities; this is consistent with the comparable hardness values attained in the SZs.

By increasing the distance from the middle line of the welding in the direction of the TMAZs, the hardness reduced. In all three samples, the lowest hardness values were measured in the TMAZs at the advancing side, in line with the results accumulated from other studies as mentioned by Yang et al., Park et al., and Lim et al. in their reports [13, 18, 20]. The hardness values would be

impacted by the crystal orientation. In the course of FSW, extreme deformations took place in the welded joint. Consequently, a special orientation distribution is generated in the FSWed samples [13, 15, 22]. Thus, the lowest hardness distribution noted in the TMAZ of the FSW AZ31B joints in the current research can be linked to crystal orientation.
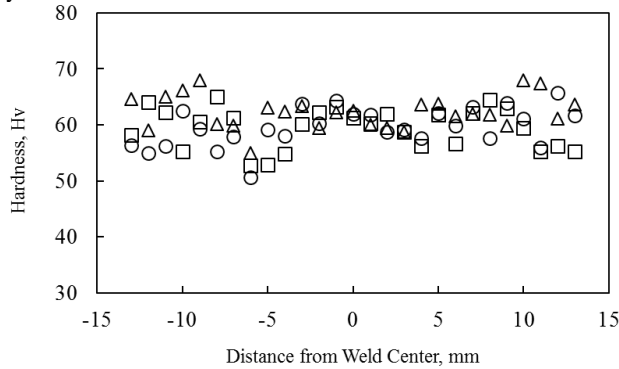
○Sample 1 - 20 mm/min △Sample 2 - 30 mm/min □Sample 3 - 40 mm/min

Fig. 9: Hardness profile of Sample 1, 2, and 3 along the middle of thickness.

Furthermore, it was noted that certain compounds were different from the base metal with macro hardness values of 90–125 HV in the SZ of Sample 1 (see Fig. 10(a)). Fig. 10(b) exhibits EDS mapping analysis carried out on portions with high microhardness values. This points out the elements disseminated, which are the key ones for the AZ31B alloy. Elemental analysis by EDS indicates that the point 1 in Fig. 10(a) has abundant Mg (1.5 % Al and 95% Mg) and point 2 possesses a constitution of 57.6% Mg and 39.9% Al. The constitution of the point 2 in the SZ almost corresponds with the $Al_{12}Mg_{17}$ intermetallic compound [23]. This intermetallic compound in the FSW of the AZ31B alloy has also been reported in recent research [24, 25].

Table 3 shows the mechanical properties of the AZ31B magnesium alloy. Yield stress, ultimate stress, and yang modulus of AZ31B were 166 MPa, 229 MPa, and 41 GPa, respectively. Furthermore, the elongation of the base metal was around 17 %. Also, The AZ31B base metal demonstrates a strain hardening behaviour along with a strain hardening coefficient of 0.29. Furthermore, the mechanical properties of the FSWed sample along with various welding travel speeds were assessed.
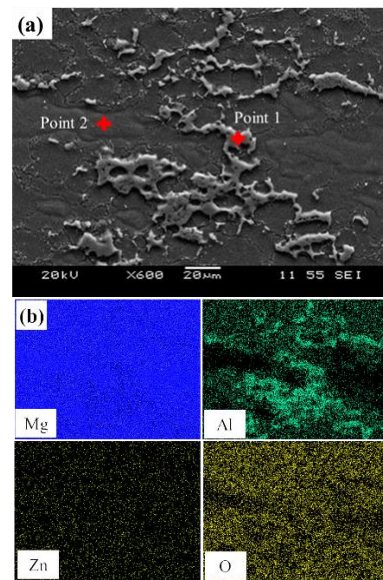
Table 3: Mechanical properties of as-rolled AZ31B Mg alloy.

Yield Stress (MPa)	Ultimate Stress (MPa)	Young's Modulus (GPa)	Elongation (%)
166	229	41	17

Table 4 shows the average of the three results of three samples in each condition. The results show that increasing the welding travel speed of 20 mm/min to 40 mm/min enabled an ultimate increase from 182 MPa to 207 MPa. Highest tensile strength (207 MPa),
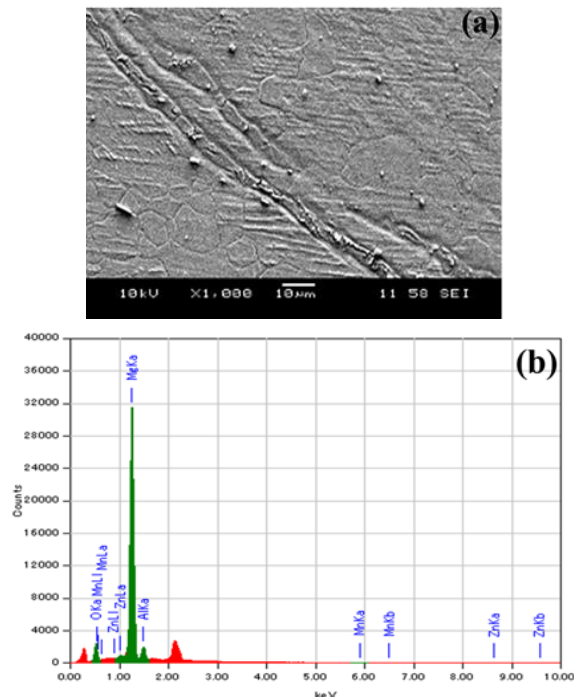

Fig. 10: SZ SEM photograph of sample 1; (a) EDS point analysis location, and (b) EDS mapping.

elongation (10 %) and welding efficiency (91%) were exhibited in the rotation speed of 700 rpm and a welding speed of 40 mm/min, which was Sample 3. It can be observed that the ultimate stress of the welded samples was lower than the for the FSWed AZ31 alloy by other researchers [5, 8, 13, 26, 27]. Moreover, the ultimate strength increase with the decrease of the ration of rotation speed to the welding travel speed (ω/υ) is similar to results obtained by previous researchers [7, 8]. In addition, the ductility level of the welded samples was significantly less (40%) than the base metals. A comparison of the tensile results of the AZ31B welded samples showed that increasing the welding speed of 20 mm/min to 40 mm/min caused an increase of the ductility level from 7.5 % to 8 %. Although the elongation values were higher in FSWed AZ31B, the elongation was not sensitive to low welding travel speed [13, 20]. Furthermore, there was a little difference in the yield stress of the FSWed AZ31B due to the altering of the welding travel speed which was about 1 %. The welding efficiency which is a ratio of tensile strength of the welded sample to base metal, varied from 83% in 20 mm/min to 91% in 30 mm/min, as well.

The fracture locations were TMAZs for samples 2 and 3 wherein plastic deformation was noted. The fracture locations in these two samples had a sound agreement with the hardness tests, which indicated that the weakest zones were the TMAZs for both. The hardness result as shown in Sample 1 was contrary to the fracture location. The lowest hardness was noted in the TMAZ; however, the fracture took place in the SZ. This shows that hardness is not the sole aspect to determine the AZ31B magnesium alloy's mechanical properties.

Figure 11 shows an EDS analysis of the fracture initiation area at the SZ of Sample 1. The results indicate the existence of an oxide layer that weakened the mechanical strength of the joint [7]. Welding efficacy is the ratio of ultimate stress of the welded sample to the ultimate stress of the base metal.

Table 4: Mechanical properties of FSWed AZ31B under different welding parameters.

Sample No.	Rotation Speed (rpm)	Travel Speed (mm/min)	Ultimate Stress (MPa)	Elongation (%)	Welding Efficiency (%)	Fracture Location
1		20	182	7.5	83	SZ
2	700	30	195	7.5	86	TMAZ
3		40	207	8	91	TMAZ

Fig. 11: (a) SEM photograph of SZ in Sample 1, (b) EDS analysis of fracture location in SZ of Sample 1.

Figure 12 shows the SEM micrographs of fracture surfaces of the FSWed samples following the tensile tests. These surfaces comprised cleavage faces, dimples, and tear ridges for the base metal as well as welded samples that were reported and scrutinised by other studies on FSWed AZ31 [7, 13, 27]. For all samples, the tear ridges were elongated on the fracture surfaces. However, the tear ridges in the fracture surface of Sample 1 that failed from the SZ were unlike the tear ridges of the base metal and fracture surfaces of samples 2 and 3.
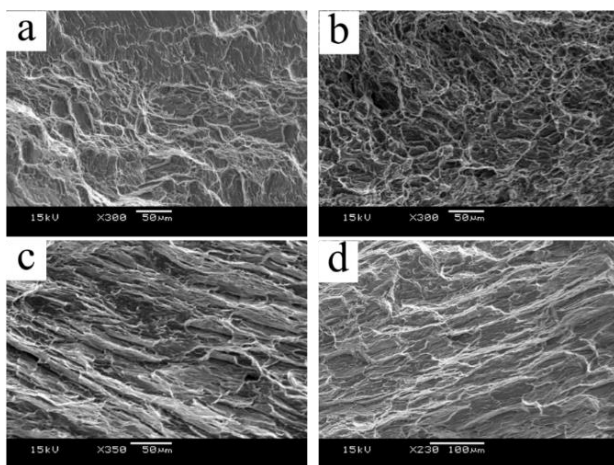
Fig. 12: Fracture surface of (a) base metal and welded samples: (b) sample 1 - 20 mm/min, (c) sample 2 - 30 mm/min, and (d) sample 3 - 40 mm/min.

4. Conclusion

On raising the welding travel speed from 20 to 40 mm/minute, the average grain size in the SZ reduced. Furthermore, the grains in the TMAZ showed a slight growth in comparing to the SZs. The three FSW samples exhibited identical hardness profiles alongside the mid-thickness of the plates, with the advanced side showing the lowest hardness in the TMAZ. By raising the welding travel speed, the tensile strength of the joints showed a tendency to grow to 207 MPa at a 40 mm/min welding travel speed. Moreover, the elongation was not considerably different in all three circumstanc-

es which were around 8 %. Welding efficiency was raised from 83% to 91% with the rise in welding travel speed. Furthermore, the fracture location was moved from the stir zone in 20 mm/min to the TMAZ in 30 mm/min.

Acknowledgement

References

[1] Singarapu U, Adepu K & Arumalle SR (2015), Influence of tool material and rotational speed on mechanical properties of friction stir welded AZ31B magnesium alloy. *Journal of Magnesium and Alloys* vol. 3, no. 4, pp. 335-344.

[2] Mordike B & Ebert T (2001), Magnesium: Properties—applications—potential. *Materials Science and Engineering*: A vol. 302, no. 1, pp. 37-45.

[3] Li W et al. (2014), Effects of tool rotational and welding speed on microstructure and mechanical properties of bobbin-tool friction-stir welded Mg AZ31. *Materials & Design* vol. 64, pp. 714-720.

[4] Park J, Kim K, Lee J & Yoon J (2015), Light-weight design of automotive suspension link based on design of experiment *International Journal of Automotive Technology* vol. 16, no. 1, p. 67.

[5] Lee WB, Yeon YM & Jung SB (2003), Joint properties of friction stir welded AZ31B– H24 magnesium alloy. *Materials Science and Technology* vol. 19, no. 6, pp. 785-790.

[6] Esparza JA, Davis WC, Trillo EA & Murr LE (2002), Friction stir welding of magnesium alloy AZ31B. Jou*rnal of Materials Science Letters* vol. 21, no. 12, pp. 917-920.

[7] Motalleb-nejad P, Saeid T, Heidarzadeh A, Darzi K & Ashjari M (2014), Effect of tool pin profile on microstructure and mechanical properties of friction stir welded AZ31B magnesium alloy. *Materials & Design* vol. 59, pp. 221-226.

[8] Abbasi Gharacheh M, Kokabi AH, Daneshi GH, Shalchi B & Sarrafi R (2006), The influence of the ratio of rotational speed/traverse speed (ω/v) on mechanical properties of AZ31 friction stir welds. *International Journal of Machine Tools and Manufacture* vol. 46, no. 15, pp. 1983-1987.

[9] Afrin N, Chen DL, Cao X & Jahazi M (2008), Microstructure and tensile properties of friction stir welded AZ31B magnesium alloy. *Materials Science and Engineering: A* vol. 472, no. 1-2, pp. 179-186.

[10] Wang YN, Chang CI, Lee CJ, Lin HK & Huang JC (2006), Texture and weak grain size dependence in friction stir processed Mg–Al–Zn alloy. *Scripta Materialia* vol. 55, no. 7, pp. 637-640.

[11] Hirano S, Okamoto K, Doi M, Okamura H, Inagaki M & Aono Y (2003), Microstructure of dissimilar joint interface of magnesium alloy and aluminum alloy by friction stir welding. *Quarterly Journal of the Japan Welding Society*.

[12] Lim S, Kim S, Lee C-G, Kim S & Yim C (2005), Tensile behavior of friction-stir-welded AZ31-H24 Mg alloy (in English). *Metallurgical and Materials Transactions: A* vol. 36, no. 6, pp. 1609-1612, 2005/06/01.

[13] Yang J, Xiao BL, Wang D & Ma ZY (2010), Effects of heat input on tensile properties and fracture behavior of friction stir welded Mg–3Al–1Zn alloy. *Materials Science and Engineering: A* vol. 527, no. 3, pp. 708-714.

[14] Mishra RS & Ma ZY (2005), Friction stir welding and processing. *Materials Science and Engineering: R: Reports* vol. 50, no. 1, pp. 1-78.

[15] Park S, Sato Y & Kokawa H (2003), Basal plane texture and flow pattern in friction stir weld of a magnesium alloy (in English). *Metallurgical and Materials Transactions A* vol. 34, no. 4, pp. 987-994, 2003/04/01.

[16] Woo W, Choo H, Brown DW, Liaw PK & Feng Z (2006), Texture variation and its influence on the tensile behavior of a friction-stir processed magnesium alloy. *Scripta Materialia* vol. 54, no. 11, pp. 1859-1864.

[17] Woo W, Choo H, Prime MB, Feng Z & Clausen B (2008), Microstructure, texture and residual stress in a friction-stir-processed

AZ31B magnesium alloy. *Acta Materialia* vol. 56, no. 8, pp. 1701-1711.

[18] Darras BM, Khraisheh MK, Abu-Farha FK & Omar MA (2007), Friction stir processing of commercial AZ31 magnesium alloy. *Journal of Materials Processing Technology* vol. 191, no. 1-3, pp. 77-81.

[19] Park S (2003), Effect of micro-texture on fracture location in friction stir weld of Mg alloy AZ61 during tensile test. *Scripta Materialia* vol. 49, no. 2, pp. 161-166.

[20] Padmanaban G & Balasubramanian V (2009), Selection of FSW tool pin profile, shoulder diameter and material for joining AZ31B magnesium alloy – An experimental approach. *Materials & Design* vol. 30, no. 7, pp. 2647-2656.

[21] Xunhong W & Kuaishe W (2006), Microstructure and properties of friction stir butt-welded AZ31 magnesium alloy. *Materials Science and Engineering: A* vol. 431, no. 1-2, pp. 114-117.

[22] Liu D, Xin R, Li Z, Liu Z, Zheng X & Liu Q (2015), The activation of twinning and texture evolution during bending of friction stir welded magnesium alloys. *Materials Science and Engineering: A* vol. 646, pp. 145-153.

[23] Singh D, Suryanarayana C, Mertus L & Chen R-H (2003), Extended homogeneity range of intermetallic phases in mechanically alloyed Mg–Al alloys. *Intermetallics* vol. 11, no. 4, pp. 373-376.

[24] Padmanaban G & Balasubramanian V (2011), Metallurgical characterization of pulsed current gas tungsten arc, friction stir and laser beam welded AZ31B magnesium alloy joints. *Materials Chemistry and Physics* vol. 125, no. 3, pp. 686-697.

[25] Padmanaban G & Balasubramanian V (2009), An experimental investigation on friction stir welding of AZ31B magnesium alloy. *The International Journal of Advanced Manufacturing Technology* vol. 49, no. 1-4, pp. 111-121.

[26] Afrin N, Chen DL Cao X & Jahazi M (2007), Strain hardening behavior of a friction stir welded magnesium alloy. *Scripta Materialia* vol. 57, no. 11, pp. 1004-1007.

[27] Commin L, Dumont M, Masse JE & Barrallier L (2009), Friction stir welding of AZ31 magnesium alloy rolled sheets: Influence of processing parameters. *Acta Materialia* vol. 57, no. 2, pp. 326-334.